CuS nanosheet grown on ZnS particle in aqueous solution at atmospheric pressure

JIE GAO, ZHANBIN QIN, YI SUN, YUN GAO*
College of Chemical Engineering, Hebei Province Key Laboratory for Environment Photocatalytic and Electrocatalytic Materials, North China University of Science and Technology, Tangshan Hebei 063210, P. R. China

We present the synthesis of CuS nanosheet grown on ZnS particle by the cation exchange reaction in aqueous solution at atmospheric pressure using waste zinc based adsorbent (mainly composed of ZnS) as raw material. We could facilely prepare CuS with CuS nanosheet or nanolayer morphology by tuning the reaction conditions. When we choose the $CuCl_2$ as the copper salt, we propose a phenomenological pathway for the formation of the CuS nanolayer via the orientated grown of ZnS nanoparticles, monolithic CuS nucleation, crystallization, oriented attachment, self assemble and Ostwald ripening process in the cation exchange reaction. The prepared CuS is characterized for the structural and morphological properties by powder X-ray diffraction (XRD), scanning electron microscopy (SEM) and transmission electron microscopy (TEM). The resulting CuS particles can be applied as photocatalyst under visible light, as well as electrode materials for batteries.

(Received August 29, 2018; accepted June 14, 2019)

Keywords: ZnS, Cation exchange, CuS, Nanosheet

1. Introduction

Semiconductor transition-metal chalcogenides have attracted much attention and research owing to their advantages in various areas, including the low solubility, fast reaction rates, potential for reuse and so on. In particular, CuS is one of important metal sulfide precipitation which has numerous studies due to specical properties and potential applications. For example, CuS, as a typical p-type transition metal sulfide, can be easily transformed into superconductor at low temperature [1]; Owning unique narrow bandgaps, CuS is suitable for photocatalytic degradation of waste water [2]. Thi Dieu Thuy [3] synthesized high quality CuS and CuS/ZnS core/shell nanocrystals and proved that CuS/ZnS core/shell systems become more efficiency photocatalytic degradation under visible light conditions. Up to now, although many research works have been focusing on carbon materials [4], a few works about reported CuS as electrode material for supercapacitors [5,6] and lithium ion batteries have been proved [7-9]. CuS exhibits high capacity, good electrical conductivity, flat discharge curves and long-cycle; it can absorb maximum solar energy, therefore, it is possible that CuS can be applied in solar cells. Weijun Ke [10] has proved that CuS is a good counter electrode for quantum dot-sensitized solar cells. CuS nanofilm with high electrical conductivity can modify solar cell [11]. Semiconducting nanoparticles with their unique properties have elicited active investigation in biomedical sciences. Shreya Goel [12] summarized that CuS nanoparticles has been to proved to be highly versatile and readily tunable for various biomedical applications.

CuS nanocrystals are different from normal ones, which exhibit excellent physical, chemical, structural and surface properties. CuS nanocrystals with different morphologies have been obtained, such as nanosheets [13], hollow spheres [2,14], rods [6], tubes [15,16], wires [5,7], flowers [3,17,18]. To date, a number of preparation approaches in literature, such as hydrothermal/solvothermal route [14,19], chemical bath deposition technique [20-22], microemulsion technique [23], chemical vapour transport technique [24], have been adopted in CuS nanoparticle synthesis. However, these above processes which consist of multiple steps are inherently complicated. It remains a challenge to achieve appropriate CuS just through simple preparation. Meantime, the particle growth mechanism of CuS is rarely studied, further investigations about impact factors are highly needed.

In recent years, copper chalcogenide have been investigated extensively in cation exchange (CE) reactions [25-27]. The cation sublattice is partially or completely exchanged by a sublattice of new types of cations, with modification of the anion sublattice in CE [28,29]. CE reactions is related to valency, ionic radius and solvation energy of the entering and exiting cations have been reported before [30]. In order to achieve extration of Cu^+ ions from the CuS is important to use phosphines (such as tributylphosphine or trioctylphosphine) in CE reactions [31,32]. Joseph M. Luther [33] sequentially employed exchange reactions to convert CdS NCs first to Cu_2S and

then to PbS. Finally, the exchange of Pb^{2+} with Cu_2S NCs is performed by adding Pb^{2+} and tributylphosphine (TBP). Haitao Zhu [34] synthesized $(Ag,Cu)_2S$ hollow microspheres with cation exchange method using spherical aggregates of CuS nanoparticles as templates. Cation exchange is a common technology which uses template to prepare chalcogenide semiconductor nanoparticles. However, all these procedures involve organic solvent or proceed at high temperature, which are difficult to be adopted in industrial production.

In this article, nano CuS was successfully synthesized through cation exchange reaction in aqueous solution under atmospheric pressure using waste zinc based adsorbent (mainly composed of ZnS) as raw material. The process is simple, environmentally, friendly and low cost with no templates, surfactants and organic solvents. Here we investigate the effect of preparation conditions on the morphology of CuS nanostructures in order to accurately control the morphology during the cation exchange reaction. This work will pave a way for the development of a low-cost and efficient method for nanomaterials.

2. Experimental

2.1. Materials

All reagents were commercially purchased from aladdin, including copper chloride dihydrate ($CuCl_2 \cdot 2H_2O$), copper nitrate dihydrate ($Cu(NO_3)_2 \cdot 3H_2O$), copper sulfate dihydrate($CuSO_4 \cdot 5H_2O$), copper (II) acetate monohydrate ($C_4H_6CuO_4 \cdot H_2O$), absolute alcohol(CH_3CH_2OH). Deionized water was used in all the experiments. All reagents were analytical grade and without further purification.

2.2. Synthesis of CuS

Firstly waste adsorbent (mainly containing ZnS) was grinded into powders by agate mortar. CuS nanoparticles were prepared by cation exchange reaction between Cu^{2+} and ZnS. In a typical preparation procedure, ZnS powder was dispersed in 150 mL of the copper salt solution (0.5 mol/L). The mixed solution was stirred for different time. we can observe that the typical blue of copper salt turned into colourless, which indicated a successful exchange. The kind of copper salt and the reaction temperature were varied for preparing different morphologies of CuS. After cooling to room temperature and filtration, the final products were rinsed with ethanol and distilled water, then dried in a vacuum oven at 60℃ for 8 h for further characterization.

2.3. Characterization

The phase structures of as-obtained CuS were analyzed by X-ray diffractometry (XRD) using a Rigaku D/MAX2500 PC diffractometer. The morphology and sizes of the samples were observed by scanning electron microscope (SEM) (Hitachi, s-4800). Transmission electron microscopy (TEM) (JEOL Ltd., JEM-2010) and Energy Dispersive Spectroscopy (EDS) elemental mapping images were recorded.

3. Results and discussion

3.1. Characterization of waste adsorbent powers

Fig. 1a shows the XRD pattern of the ZnS powder which come from desulfurization. All diffraction peaks match well with the standard pattern of wurtzite ZnS (JCPDS NO. 36-1450) without other impurity. From the line width of the (100) reflection, the Scherrer equation $D = K\lambda/(\beta\cos\theta)$, with D being the crystallite size, λ the X-ray wavelength, β the full width at half-maximum of the diffraction peak, θ the Bragg angle, and K = 0.89, yields a crystallite coherence length of 33.0637 nm along the (100) direction. According to the Scherrer equation, the average crystalline size is calculated to be 41.039 nm. The ZnS products are well crystalline because of the sharp diffraction peaks in nature. The main diffraction peaks are observed at about 2θ=26.914°, 28.500°, 30.527°, 47.561°, 51.776°, 55.500°and the corresponding lattice planes could be indexed to (100), (002), (101), (110), (103), (200) as in accordance with the standard card. It indicates that ZnS exists as wurtzite phase. Typical SEM images is shown in Fig. 1b, the nanoflakes next to each other with a size of about 100 nm.

The EDS pattern (Fig. 1c-e) of the product clearly revealed that it consisted of mainly Zn and S elements. The atomic ratio of Zn to S is approximate 1:1, confirming the stoichiometry of ZnS.

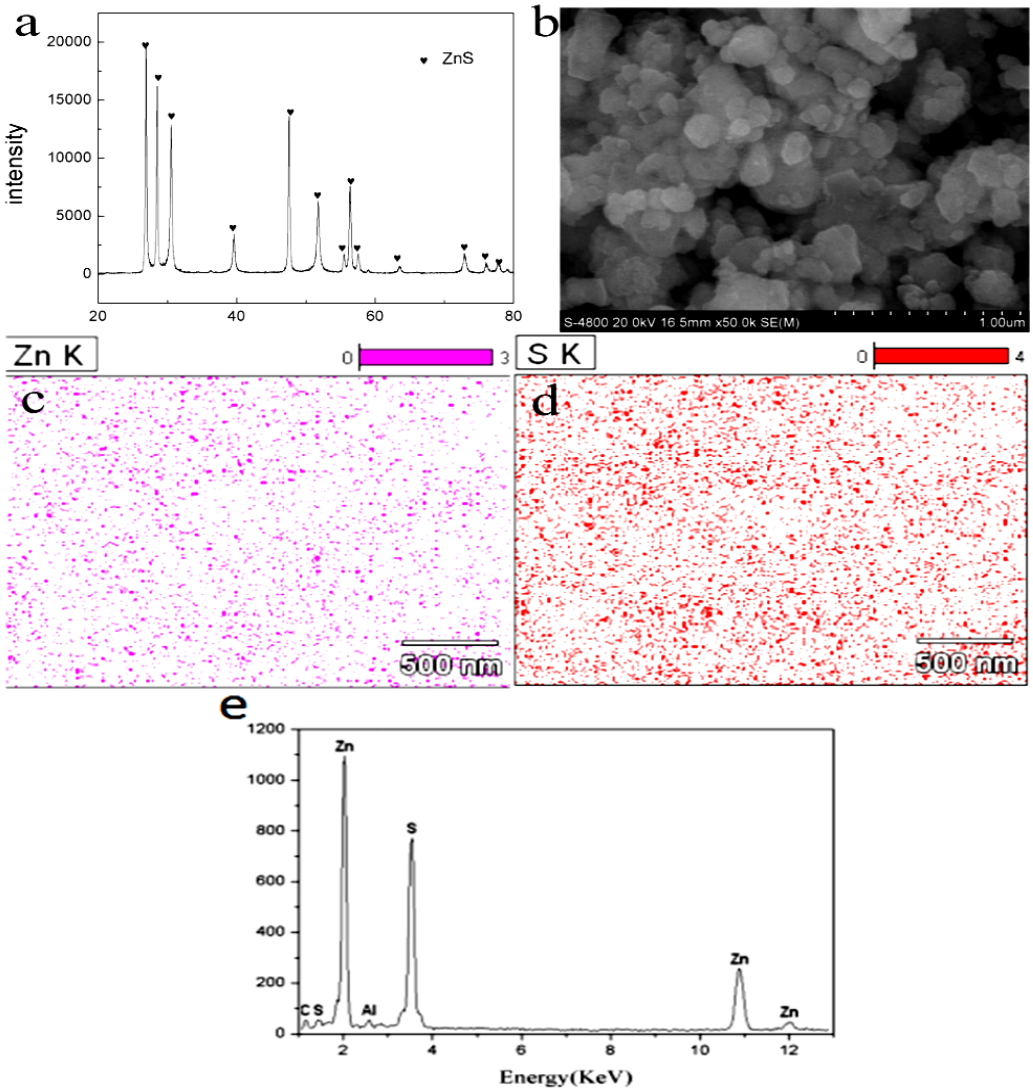

Fig. 1. XRD pattern of ZnS power (a); SEM image of ZnS powder (b); EDS image of element distribution (c,d,e)

3.2. The influence factor of synthesizing CuS

A systematic investigation on the synthesis of CuS nanocrystals has been made by cation exchange reaction as mentioned in the experimental section. The effect factors of as-obtained CuS were studied in detail using scanning electron microscope (SEM) and X-ray diffraction (XRD).

Firstly, the effect of copper salt types on the morphology of the products was investigated. Fig. 2a. shows the XRD image of the CuS synthesized at 100℃ for 24 h with different copper salt types. When $CuSO_4$ and $CuCl_2$ are selected, the XRD pattern (Fig. 2) shows that almost all diffraction peaks can be indexed to the hexagon phase of CuS (covellite type, space group P63/mmc) with the lattice parameters of a = 3.792 Å and c = 16.344 Å (JCPDS No. 06-0464). The ZnS is completely converted to CuS. However, the shape of diffraction peaks is different from $CuSO_4$ and $CuCl_2$. When the copper salt is $CuSO_4$, it can be seen that diffraction peaks of CuS products become narrower and stronger, compared with $CuCl_2$. These results demonstrate an increase in the crystallinity and the average crystallite size. On the contrary, imply a decrease in the crystallinity with the widths of peaks. When $Cu(NO_3)_2$ or $Cu(Ac)_2$ is selected, it can be seen from Fig. 2a that ZnS and CuS and a Cu_9S_5 in the sample are identified from their standard diffraction peaks. Obviously, the XRD peak intensities of ZnS within the composite become weak, implying a particle transformation of ZnS. The morphology of CuS product is characterized by SEM and presented in Fig. 3. Fig. 3a-c shows the SEM images of the products obtained from ZnS and different copper salts whose molar ratio of is 1: 1. In this synthesis, when $Cu(NO_3)_2$, $CuSO_4$, $Cu(Ac)_2$ are used as the copper salt, the nanosheet of CuS were fabricated, respectively (Fig. 3a,b and c). Fig. 3b shows some CuS nanosheets appear to be agglomerated and the morphology with large size. However, when using $CuCl_2$ as copper salt, the synthesis resulted in the formation of nanolayered CuS (Fig. 3d). These nanolayered consist of nanosheet in the size about 100 nm. Generally, the type of the copper salt can influence the morphology of CuS.

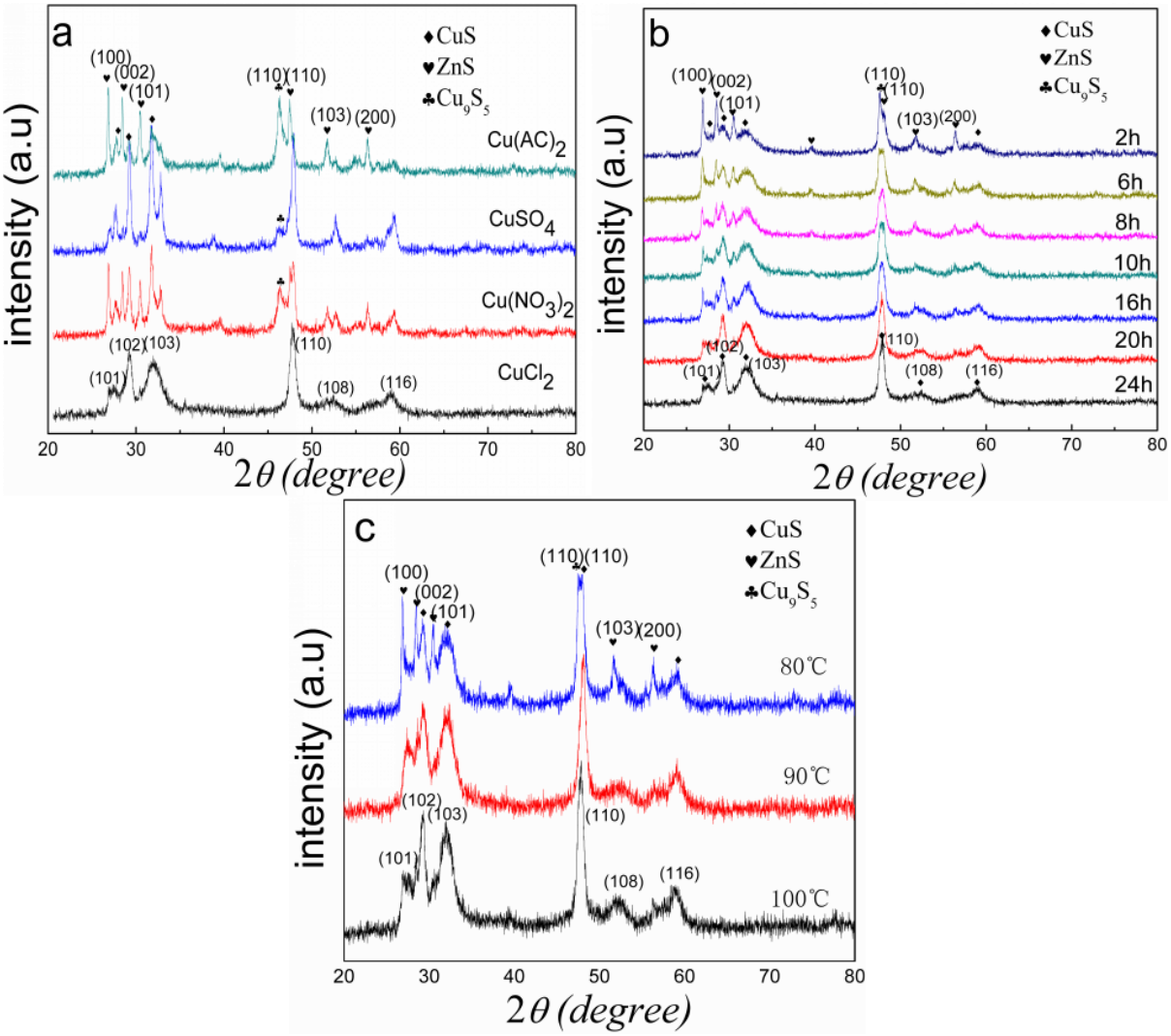

Fig. 2. XRD patterns of as-obtained CuS products synthesized with different (a) copper salt types, (b) reaction temperatures and (c) reaction times

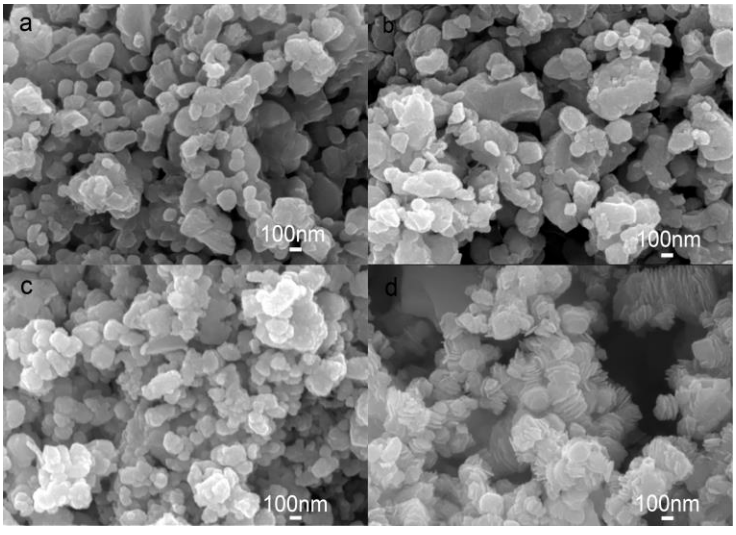

Fig. 3. SEM image of as-obtained CuS from different copper salt: (a) $Cu(NO_3)_2$, (b) $CuSO_4$, (c) $Cu(Ac)_2$, (d) $CuCl_2$

To study the influences of reaction temperature on the morphology of CuS, experiments were designed to keep all other parameters such as precursor molar ratio ($CuCl_2$:ZnS) = 1:1, the concentration of $CuCl_2$ (0.5 mol/L), reaction duration (8 h) fixed. Compared with the standard XRD pattern for CuS, when the reaction temperature is up to 90 ^oC, all diffraction peaks are almost CuS (Fig. 2b). With the synthesis temperature increasing, the XRD peaks of CuS became stronger and stronger, confirming that more and more CuS are formed. This result indicates that high temperature could enhance the exchange rate between Cu^{2+} and Zn^{2+}.

In order to understand the effect of reaction time, experiments were designed to keep the concentration of 0.5 mol/L and the reaction temperature of 100 ^oC. After the reaction was allowed for a specific duration, the reaction vessel was cooled down to room temperature and the product was collected by filter. Fig. 2c shows the XRD patterns of the products synthesized in $CuCl_2$ solution with different reaction time. It can be seen that the reaction time is critical to synthesize CuS. When the reaction time duration is 2 h, there are bits of diffraction peaks which can be indexed to the hexagonal CuS (JCPDS6-0464). However, all diffraction peaks of intensity are low and the shape of peaks are obvious width. So it indicates that the size of CuS is small in the initial reaction stage. With the prolongation of reaction time, the diffraction peaks show stronger intensity which indicates that the crystallinity of the products will be improved with time. When the reaction time is 24h, the XRD pattern only showed pure CuS (Fig. 2c), revealing a complete phase transition into CuS [13], which means all of the Cu^{2+} will finally enter the lattice of the ZnS and exchange Zn^{2+} out. Therefore, it can be concluded that reaction time has great influence on the CuS products.

3.3. A possible formation mechanism of layered CuS

We choose $CuCl_2$ as copper salt to substantially understand the growth mechanism of copper sulfide nanolayer structure. The grain growth process of as-synthesized CuS was examined by TEM and SEM. The nanolayer morphology evolution can be seen from Fig. 4a to Fig. 4c. As shown in the SEM image (Fig. 4a,b), it can be seen that the nanosheet is produced not along the surface but perpendicular to the surface of these aggregated large particles. The XRD pattern shows both ZnS and CuS coexist in the composites. The particle diffraction peaks of pure CuS correspond to (JCPDS6-0464) with the P63/mmc space group and a primitive hexagonal unit cell with a=3.792 and c=16.344, as shown in Fig. 4d. Differences in the diffraction peaks were observed when compared with the standard pattern. For instance, the intensity of the (103) peak is lower than the standard card and all these peaks are broadened. This indicates that the growth of the certain crystallographic plane form special morphology. From the XRD pattern, the intensity of the (110) peak is obviously strong, this make the preferential growth which is prefer to form hexagonal CuS nanosheets clearly.

The TEM images of the nanoparticles synthesized at 100 ^oC for 6h with $CuCl_2$ are shown in Fig. 5. Fig. 5a shows that most of the particles are nanosheets with a few nanolayers. The size of the particles is about 100 nm. However, careful observation reveals that the nanostructure of the one-dimensional structures are, in fact, the hexagonal nanoplates of CuS. Therefore, we can infer that the monolithic of nanosheet which is perpendicular to the surface of bluck is the hexagonal nanoplates of CuS. The TEM image (Fig. 5b) shows some nanosheets stack together. It can be seen CuS nanosheet tend to assemble into nanolayer. The inside of Fig. 5b shows the energy dispersive X-ray (EDX) spectra of CuS, The Cu to S atomic ratio for all these cases is found to be approximately 1:1, confirming stoichiometry of CuS. The distance between two neighboring fringes is about 0.28 nm, which is consistent with the (103) plane of the hexagonal covellite CuS as shown in Fig. 5c. The spot selected area electron diffraction (SAED) pattern (Fig. 5d) suggests the single-crystalline nature of individual nanoparticle in the CuS.

At the initial reaction stage, ZnS powder is dispersed in copper salt solution. The solubility of ZnS product is 1.6×10^{-24}. As given in Eq.(1), there is a small amount of Zn^{2+} and S^{2-} ions existing in the reaction solution around the solid ZnS due to the dynamic equilibrium. When the Cu^{2+} is added to the vessel, there are a lot of Cu^{2+} combine with S^{2-} to form CuS deposited on the surface of ZnS by the heterogeneous nucleation (Eq.(2)). The other Cu^{2+} adsorb on the surface of ZnS. The CuS nanoparticles are in situ formed on the ZnS surface, which can avoid the quick nucleation and growth of CuS in the solution. It is expected that there are two main chemical reactions existing during this phase and morphological evolution, which are given as follows:

$$ZnS \Leftrightarrow Zn^{2+} + S^{2-} \quad (1)$$

$$Cu^{2+} + S^{2-} \Leftrightarrow CuS \quad (2)$$

The solubility product constant (Ksp) of ZnS and CuS is 1.6×10^{-24} and 6.3×10^{-36}, respectively. Such large difference in solubility provides the driving force for cation exchange. According to the literature [35] reported the cation exchange reaction between Hg^{2+} and ZnS NCs, it can be seen that the Hg^{2+} concentration decreased quickly; about 99.9%, Hg^{2+} is removed by the ZnS NCs sorbent in 60 s. However, the Zn^{2+} concentration increased slowly. Obviously, only part of Hg^{2+} is removed through cation exchange, the other part of Hg^{2+} is possibly adsorbed by the surface of ZnS NCs sorbent at 60 s. With

the extension of reaction time, the ZnS nanoparticles gradually dissolved and recrystallized, and the ZnS nanoparticles in situ nucleate and preferentially grow on the surface of the nanparticles. Accorrding to the equation of Q = (C-S)/S, when the concentration of Zn^{2+} is low, it is benefit to the orientated growth of ZnS nanoparticles. If the rate of nucleation and growth of the nanocrystals is constant throughout the aggregation process, so aggregate size increases due to the supply of primary particles compensates for their consumption. The important observation is made on the ZnS structures in Fig. 4a,b, the length and diameter of the ZnS structures are increased and the surface is smooth. Simultaneously, with the cation exchange is ongoing, the ZnS has a strong tendency to dissolve due to the reduction of S^{2-} concentration in the solution and its added CuS. When the concentration of Zn^{2+} increase, the aggregation rate is larger than the rate of orientated growth, the size of ZnS is no longer magnify.

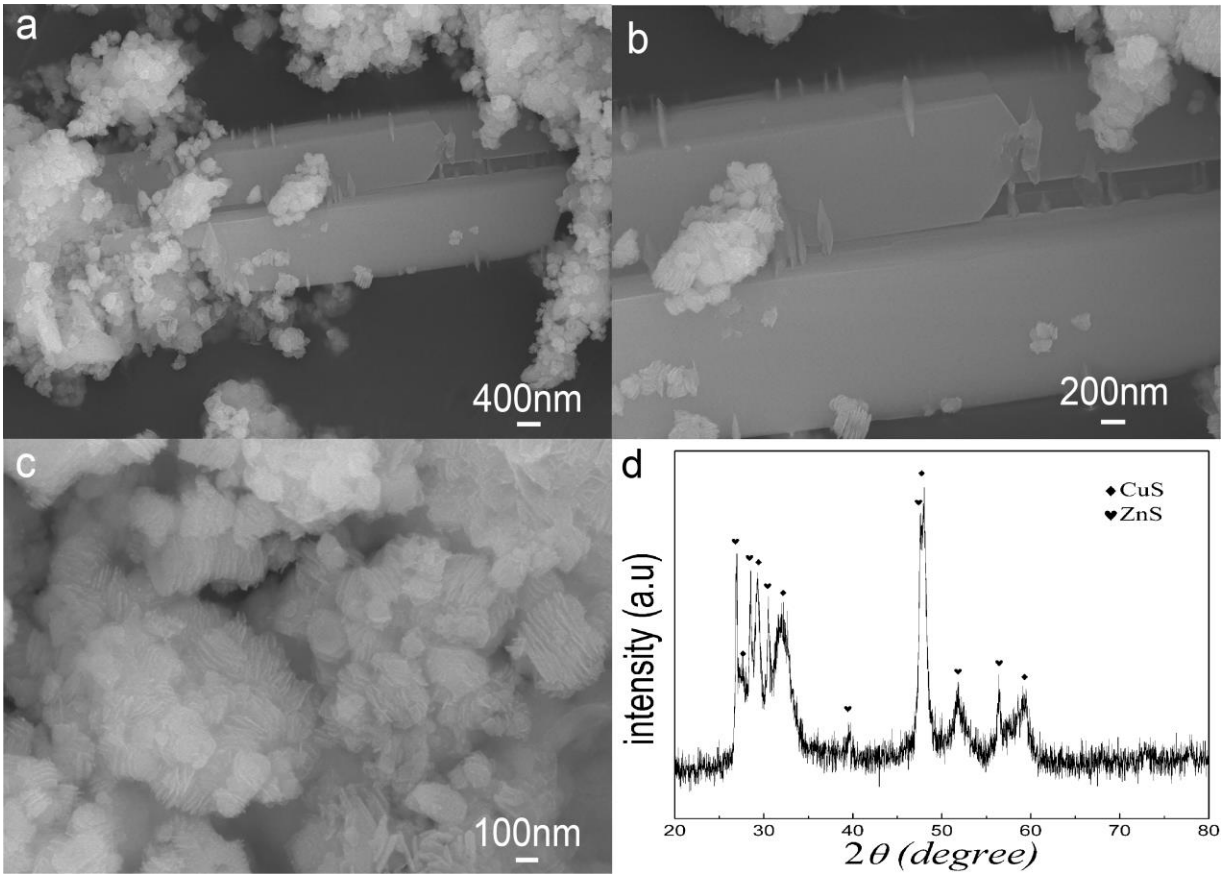

Fig. 4. SEM image (a, b, c) and XRD (d) patterns of as-obtained CuS

As shown in the SEM image (Fig. 4b), it can be seen the monolithic of CuS is nucleating and growing on the surface of ZnS which has aggregated into large particles. On the basis of this research, the nanolayered CuS was found to be assembled of either nanoplates or nanoparticles [36]. Consequently, with the reaction continue, we can understand CuS nanosheet tend to assemble into nanolayer and agglomerate together (Fig. 5e,f). Between the layers there exists so weak van der Waals force and covalent bonds that crystals can easily cleave and obtain smooth surface [37]. In addition, the flake-like crystals can orientiated attachment and self-assemble into steady stratiform CuS due to the minimization of the interfacial free energy by reducing the surface areas. There are a large number of about Ostwald ripening [38, 39]. Ripening involves interparticle transport of mobile species, with larger particles growing at the expense of smaller particles due to the differences of in surface energy [40]. When the stratiform CuS increase, it falls off gradually.

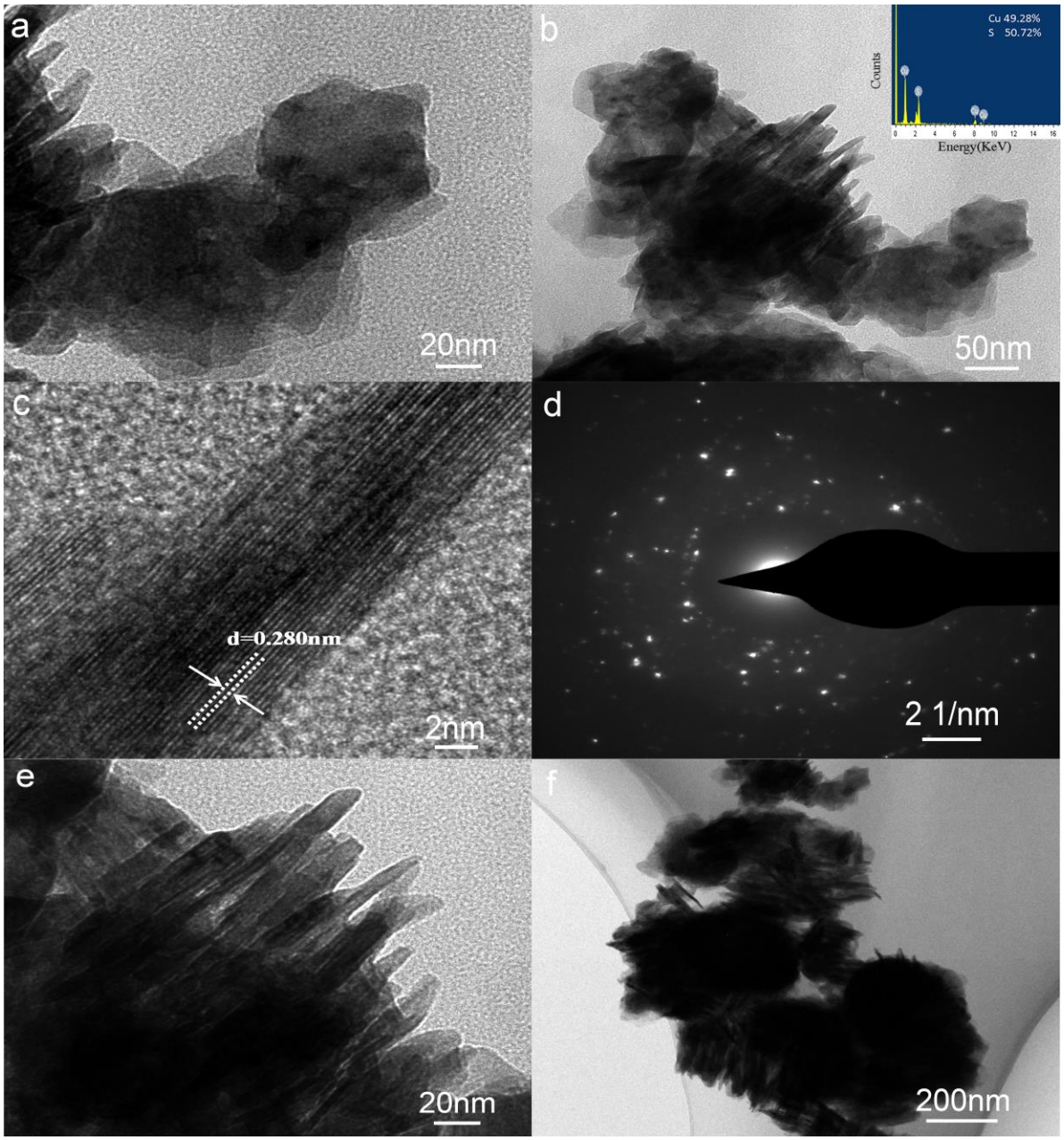

Fig. 5. TEM image of as-obtained CuS

On the basis of the above-mentioned observations, the formation mechanism of the CuS nanolayer is proposed in Fig. 6. In the initial stages, the ZnS nanoparticles orientated growth, meanwhile, CuS crystal is nucleated on the surface of ZnS. With the extension of reaction time, the CuS begin to crystallize and orientated attachment. Then, the CuS nanosheet self-assemble into nanolayer due to van der Waals force and fall off gradually.

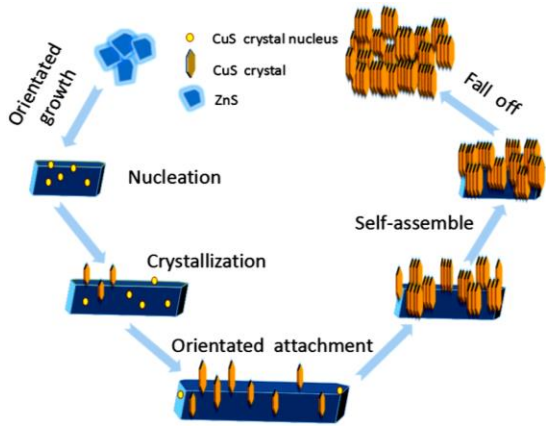

Fig. 6. Schematic illustration of the formation and shape evolution of the CuS nanolayer in the whole synthetic process

4. Conclusion

In summary, the hexagonal nanolayered CuS were successfully synthesized through cation exchange method in aqueous solution under atmospheric pressure using waste zinc based adsorbent (mainly composed of ZnS) as raw material. The influence factors are discussed based on the results of XRD and SEM. The detail structural study has revealed that the cation exchange proceeds to form CuS nanolayer. It can be seen that the type of copper salt plays an important role in controlling the morphologies of the CuS crystals in their self-assembling process. Obviously, the van der Waals forces between the hexagonal CuS nanosheets can promote the oriented attachment. This mechanism on synthesizing nanolayered CuS may spark a further investigation.

Acknowledgments

The work was financially supported by the Natural Science Foundation of Hebei Province of China (No. E2017209175).

References

[1] U. Shamraiz, R. A. Hussain, A. Badshah, Journal of Solid State Chemistry France **238**, 25 (2016).
[2] J. Yu, J. Zhang, S. Liu. Journal of Physical Chemistry C **114**, 13642 (2010).
[3] U. T. D. Thuy, N. Q. Liem, C. M. A. Parlett, G. M. Lalev, K. Wilson, Catalysis Communications **44**, 726101 (2014).
[4] Y. Long, Z. Chen, X. Zhang, J. Zhang, Z. Liu, Applied Physics Letters **85**, 1796 (2004).
[5] Y. K. Hsu, Y. C. Chen, Y. G. Lin, Electrochimica Acta **139**, 401 (2014).
[6] J. Zhang, H. Feng, J. Yang, Q. Qin, H. Fan, C. Wei, ACS Applied Materials and Interfaces **7**, 39 (2015).
[7] C. Feng, L. Zhang, M. Yang, X. Song, H. Zhao, Z. Jia, ACS Applied Materials and Interfaces **7**, 29 (2015).
[8] M. Zhou, N. Peng, Z. Liu, Y. Xi, H. He, Y. Xia, Journal of Power Sources **306**, 408 (2016).
[9] Y. Han, Y. Wang, W. Gao, Y. Wang, L. Jiao, H. Yuan, Powder Technology **212**, 64 (2011).
[10] W. Ke, G. Fang, H. Lei, P. Qin, T. Hong, W. Zeng, Journal of Power Sources **248**, 809 (2014).
[11] H. Lei, P. Qin, W. Ke, Y. Guo, X. Dai, Z. Chen, Organic Electronics **22**, 173 (2015).
[12] S. Goel, F. Chen, W. Cai, Small **10**, 631 (2014).
[13] J. Zhang, J. Yu, Y. Zhang, L. Qin, R. G. Jian, Nano Letters **11**, 4774 (2011).
[14] K. J. Huang, J. Z. Zhang, Y. Liu, Y. M. Liu, International Journal of Hydrogen Energy **40**, 10158 (2015).
[15] J. Huang, Y. Wang, C. Gu, M. Zhai, Materials Letters **99**, 31 (2013).
[16] Z. Hai, J. Huang, H. Remita, J. Chen, Materials Letters **108**, 304 (2013).
[17] Q. Wang, Y. Shi, L. Pu, Y. Ta, J. He, S. Zhang, Applied Surface Science **367**, 109 (2016).
[18] K. Mageshwari, S. S. Mali, T. Hemalatha, R. Sathyamoorthy, P. S. Patil, Progress in Solid State Chemistry **39**, 108 (2011).
[19] J. Zou, J. Jiang, L. Huang, H. Jiang, K. Huang, Solid State Sciences **13**, 1261 (2011).
[20] C. J. Raj, B. C. Kim, W. J. Cho, W. G. Lee, Y. Seo, K. H. Yu, Journal of Alloys and Compounds **586**, 191 (2014).
[21] Y. Lu, M. Xu, G. Yi, J. Jia, Journal of Colloid and Interface Science **356**, 726 (2011).
[22] M. Xu, H. Wu, P. Da, D. Zhao, G. Zheng, Nanoscale **4**, 1794 (2012).
[23] J. N. Solanki, R. Sengupta, Z. V. P. Murthy, Solid State Sciences **12**, 1560 (2010).
[24] S. H. Chaki, J. P. Tailor, M. P. Deshpande, Materials Science in Semiconductor Processing **27**, 577 (2014).
[25] L. Xiao, H. Chen, J. Huang, Materials Research Bulletin **64**, 370 (2015).
[26] X. Yi, G. Bertoni, A. Riedinger, A. Sathya, M. Prato, S. Marras, Chemistry of Materials **27**, 7531 (2015).
[27] X. M. Suai, W. Z. Shen, X. T. Li, Z. Y. Hou, S. M. Ke, G. Shi, C. L. Xu, D. H. Fan, Materials Science and Engineering B **227**, 74 (2018).
[28] R. D. Robinson, B. Sadtler, D. O. Demchenko, C. K. Erdonmez, L. W. Wang, A. P. Alivisatos, Science **317**, 355 (2007).
[29] H. S. Dong, S. M. Hughes, Y. Yin, A. P. Alivisatos, Science **306**, 1009 (2004).
[30] L. D. Trizio, H. Li, A. Casu, A. Genovese, A. Sathya, G. C. Messina, Journal of the American Chemical Society **136**, 16277 (2014).
[31] H. Li, R. Brescia, M. Povia, M. Prato, G. Bertoni, L. Manna, Journal of the American Chemical Society **135**, 12270 (2013).
[32] S. Gupta, S. V. Kershaw, A. L. Rogach, Advanced Materials **25**, 6923 (2013).
[33] J. M. Luther, H. Zheng, B. Sadtler, A. P. Alivisatos, Journal of the American Chemical Society **131**, 16851 (2009).
[34] H. Zhu, L. Chao, D. Wu, Materials Chemistry and Physics **127**, 24 (2011).
[35] Z. Qu, L. Yan, L. Li, J. Xu, M. Liu, Z. Li, ACS Applied Materials and Interfaces **6**, 18026 (2014).
[36] J. Kundu, D. Pradhan, ACS Applied Materials and Interfaces **6**, 1823 (2014).
[37] X. P. Shen, H. Zhao, H. Q. Shu, H. Zhou, A. H. Yuan, Journal of Physics and Chemistry of Solids **70**, 422 (2009).
[38] V. P. Zhdanov, Surface Science **644**, 191 (2015).
[39] D. V. Alexandrov, Journal of Physics and Chemistry of Solids **91**, 48 (2015).
[40] T. W. Hansen, A. T. Delariva, S. R. Challa, A. K. Datye, Accounts of Chemical Research **46**, 1720 (2013).

*Corresponding author: gaoyunhuagong@126.com